



Original Paper

Geochemical, mineralogical, and petrological analyses for the interpretation of the sedimentary environment of the Middle-Late Ordovician Majiagou Formation (northern China) as a tool for more effective gas exploration

Jie Gao ^a, Da-Wei Lv ^{a, b, *}, A.J. (Tom) van Loon ^c, Dun Wu ^d^a Shandong Provincial Key Laboratory of Depositional Mineralization and Sedimentary Minerals, Shandong University of Science and Technology, Qingdao, Shandong, 266590, China^b Laboratory for Marine Mineral Resources, Qingdao National Laboratory for Marine Science and Technology, Qingdao, Shandong, 266071, China^c College of Earth Science and Engineering, Shandong University of Science and Technology, Qingdao, Shandong, 266590, China^d Exploration Research Institute, Anhui Provincial Bureau of Coal Geology, Hefei, Anhui, 230088, China

ARTICLE INFO

Article history:

Received 2 November 2021

Received in revised form

6 March 2022

Accepted 3 June 2022

Available online 8 June 2022

Edited by Jie Hao

Keywords:

Majiagou Formation

Middle Ordovician

Major-element analysis

REE analysis

Trace-element analysis

Hydrocarbon exploration

ABSTRACT

Core samples from the deeply buried Ordovician Majiagou Formation below the Huainan Coalfield (E China) have been investigated for their carbonate types, major and trace elements (including rare earth elements) and C and O isotopes. The objective was to get a better insight into the possible occurrences of gas (and possibly oil) derived from Carboniferous coals. It was found that the carbonates are dolomites with strongly varying amounts of CaO and MgO. The low concentrations of SiO₂, Al₂O₃, and Fe₂O₃ indicate deposition in a normal marine environment with little terrigenous input. The Na₂O/K₂O, Fe/Mn and Sr/Ba ratios, as well as the Ga values indicate mainly a marine salinity and a hot and humid climate. The slight depletion of Ce and Eu, the depletion of heavy rare earth elements (HREE) and the enrichment of light rare earth elements (LREE) indicate deposition in a reducing environment. It thus appears that the Majiagou Formation below the Huainan Coalfield closely resembles that in the eastern part of the Ordos Basin, where several gas reservoirs are present, so that the Majiagou Formation under the Huainan Coalfield represents a promising target for hydrocarbon exploration.

© 2022 The Authors. Publishing services by Elsevier B.V. on behalf of KeAi Communications Co. Ltd. This is an open access article under the CC BY-NC-ND license (<http://creativecommons.org/licenses/by-nc-nd/4.0/>).

1. Introduction

The Middle Ordovician Majiagou Formation was deposited on the North China Block (also known as the Sino-Korean Block) and consists of thick carbonates (Meng et al., 1997; Tian and Xiao, 2013), which have been studied frequently (e.g., Meng et al., 1997; Wang and Sun, 2013; Huo et al., 2014; Su et al., 2017). These studies focused, however, on the northern part of the North China Block (see also Wang et al., 2018; Xue, 2018), and most of these studies

deal with the diagenetic characteristics (e.g., Tian and Xiao, 2013; Huo et al., 2014; Wei et al., 2017; Liu et al., 2020; Xiong et al., 2020), the lithology (Xue, 2018), the geochemistry, sedimentology, C and O isotopes, etc., particularly in the Ordos Basin (see, among others, Fu et al., 2021; Su et al., 2021) and its adjacent areas in the central part of the North China Block.

The main objective of almost all above studies was the collection of data that would help efficient and effective exploration for gas (derived from Carboniferous coal) and possibly oil. This can be done by determining the sedimentary environment in which a specific rock unit is deposited, and by reconstructing the various facies and their characteristics during sedimentation. For example, the Sr/Ba ratio and the Ga content of trace elements can be used to distinguish the continental or marine conditions that prevailed during accumulation of carbonate rocks. Taking the Majiagou Formation as an example, this formation must have been deposited in a normal

* Corresponding author. Shandong Provincial Key Laboratory of Depositional Mineralization and Sedimentary Minerals, College of Earth Sciences and Engineering, Shandong University of Science and Technology, Qingdao, Shandong, 266590, China.

E-mail addresses: m17692476182@163.com (J. Gao), lvdawei95@sdu.edu.cn (D.-W. Lv), Geocom.VanLoon@gmail.com (A.J. van Loon), wudun@ustc.edu.cn (D. Wu).

marine environment. This is consistent with earlier studies (He et al., 2014; Bao et al., 2017; Wang et al., 2018). The Mg/Ca, Sr/Ca and Mn/Sr ratios can also be used to determine the alteration and diagenesis of carbonate rocks (Derry et al., 1989; Kim et al., 1999; Averyt et al., 2003; Bayon et al., 2007; Tian, 2016; Wei et al., 2017; Liu et al., 2020; Xiong et al., 2020). Terrigenous influence can be determined by major elements, viz. through the Fe_2O_3 , Al_2O_3 and SiO_2 ratios (Wang et al., 2018); the $\text{Na}_2\text{O}/\text{K}_2\text{O}$ ratio provides information about the salinity (Gerdes et al., 2002; Huang et al., 2008). The study of the stable C and O isotopes in carbonate rocks is also widely used for the quantitative interpretation of the salinity and the water temperature during deposition, as well as for analysis of the diagenetic environment and the resulting alterations (Land and Hoops, 1973; Spielhagen and Erlenkeuser, 1994; Garcés et al., 1995; Wang and Al-Aasm, 2002; Gillikin et al., 2006; Baghdady et al., 2017; Nicolas et al., 2018; Liu et al., 2020; Xiang et al., 2020). These studies have provided a wealth of useful information for the petroleum and gas exploration.

Analysis of rare earth elements (REE) has nowadays become a useful tool to reconstruct the depositional environment of carbonates. Su et al. (2017) deduced that sea water percolating through the Majiagou Fm. must have been responsible for the dolomitization of the carbonates that initially were limestones, because Eu shows no positive anomaly that might be explained by the influx of meteoric water through karstic limestone. Xiang et al. (2020) found in their geochemical study of major elements, trace elements, rare earth elements and the stable isotopes of carbon, oxygen and strontium in the Majiagou Fm. that the dolomite was formed under high-temperature burial conditions, and that the dolomitizing fluids had all a similar origin/source.

Relatively few studies concern the Majiagou Formation in the southern part of the North China Block because of its deep burial. Most of them deal with the environment in which the vegetation that changed into coal developed, and with the climate at the time (Sun et al., 2010; Li et al., 2013; Han et al., 2015; Chen et al., 2018; Munir et al., 2018; Wang, 2020; Zhang et al., 2021). The present study aims at revealing the characteristics of the sedimentary environment of the deeply-buried Majiagou Fm. on the southern part of the North China Block by geochemical, petrological and mineralogical investigation of cores obtained from the Majiagou carbonates by the drilling of a well below the Huainan Coalfield.

2. Geological setting

The study area is situated in the southeastern corner of a giant Carboniferous–Permian coal-accumulating depression in the Huainan area in northern China (Fig. 1). Tectonically this is in the southern margin of the North China Block. The southern margin of the North China Plate is mainly controlled by the orogeny of the Qinling–Dabie orogenic belt. This belt and its adjacent areas have experienced a long and complex evolutionary history. It is a complex continental orogenic belt, formed by the subduction of the North China Plate during its collision with the South China Plate (also called the Yangtze Plate) and the Qinling Plate. During the Late Paleozoic, the southern margin of North China became an active continental margin due to the subduction of the Yangtze Plate under the North China Plate (Ma, 2008). The subsidence center of the North China Plate moved southwards. A small high was formed in the north of Huainan. With the change of the global sea level, extensive and thick delta deposits formed in the Huainan Basin in the southern part of North China. The Huainan Basin is bound in the south by the Mesozoic Hefei Depression, in the north by the Bengbu–Taihe High, in the west by the Mesozoic–Cenozoic Zhoukou Depression, and in the east by the Tanlu Fault Zone (Fig. 1).

The rocks under study constitute the upper half of the Middle

Ordovician Majiagou Formation below the Huainan Coalfield; the formation consists of carbonate rocks that form a succession between the overlying Permo–Carboniferous Taiyuan Formation and the underlying Cambrian Tuba Formation. The Majiagou Formation has been studied, sampled and analyzed previously, but almost exclusively in the Ordos Basin. We compare our findings with those of Wang et al. (2018), because of the comparable setting, but also to find out whether the rocks under study here, which are buried deeply below the Huainan Coalfield, could – in principle – house hydrocarbon reservoirs like the equivalent rocks in the eastern part of the Ordos Basin studied by Wang et al. (2018), which are buried much less deeply. This difference in depth may have had implications for the origination and preservation of hydrocarbons, so that it is of great scientific and economic importance to compare the formation in these two areas (Fig. 2). This is done primarily on the basis of the petrological composition, the contents of major and trace elements, and the anomalies in the concentrations of the stable carbon and oxygen isotopes.

In the study area, the top part of the Majiagou Formation consists mainly of light grayish green and dark red carbonates with some grayish parts. The carbonates are cryptocrystalline with well-developed primary fissures and equally well-developed cement. Downwards the color becomes grayish to grayish green due to the presence of more clayey material and it becomes finer cryptocrystalline. The lowermost part of the Majiagou Formation is light white and yellow, and the unweathered surface is fleshy red, and the rocks are still cryptocrystalline.

Three samples (Fig. 2) were collected from the Majiagou Formation for analysis. The samples are a dolomite (sample SO1), a dolomitic limestone (sample SO2) and a calcareous dolomite (sample SO3). The names of the rock types are based on the CaO/MgO ratio (cf. Chilingar, 1960; Feng, 1993): if the ratio is > 50.1 , a sample is named 'limestone'; if the ratio is 4.0–50.1, it is named 'dolomitic limestone'; if the ratio is 1.5–4.0, it is named 'calcareous dolomite'; and if the ratio is < 1.5 , it is named 'dolomite'.

Element analysis makes it possible, in combination with thin-section analysis of the samples, to reconstruct the geochemical and paleoenvironmental characteristics of the dolomites. Comparison of these results with the geochemical characteristics of three representative and petrologically comparable reference samples (ZJ4, a dolomite; ZJ14, a dolomitic limestone; and ZJ24, a calcareous dolomite) collected by Wang et al. (2018) from correlatable levels of the Majiagou Formation in the eastern margin of the Ordos Basin (Fig. 2) provides insight into the environment of the formation where buried below the Huainan Coalfield. This is particularly of interest because the Majiagou Formation had not been drilled and sampled before in the Huainan Basin and also because only few data are available about this formation from outside the Ordos Basin. Consequently, important new information could thus be obtained that will be helpful for future oil and gas exploration in the southern part of the North China Block.

3. Materials and methods

3.1. Sample collection and preparation

Dolomite samples from the middle and upper parts of the Majiagou Formation were collected from borehole Y2 in the Huainan Coalfield (Fig. 2). Three cores were obtained: a lower one with a length of 6.9 m (with a recovery of 86%), an intermediate one (length 9.9 m, recovery 96%), and an upper one (length 8.5 m, recovery 96%). From each of these cores, a representative sample was taken, coded SO1, SO2, and SO3, respectively (Fig. 2). The parts of the samples that were not selected for analysis were stored in airtight self-sealing bags and placed in dryers to protect the

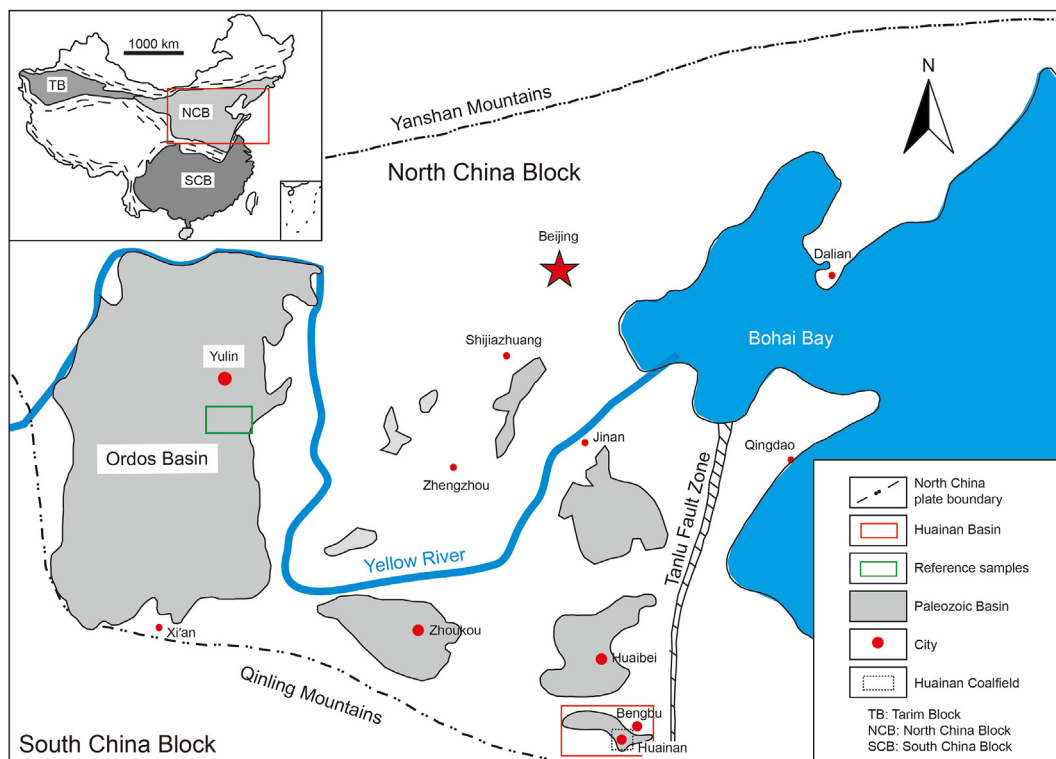


Fig. 1. Location of the Huainan Coalfield within China. Inset: tectonic setting.

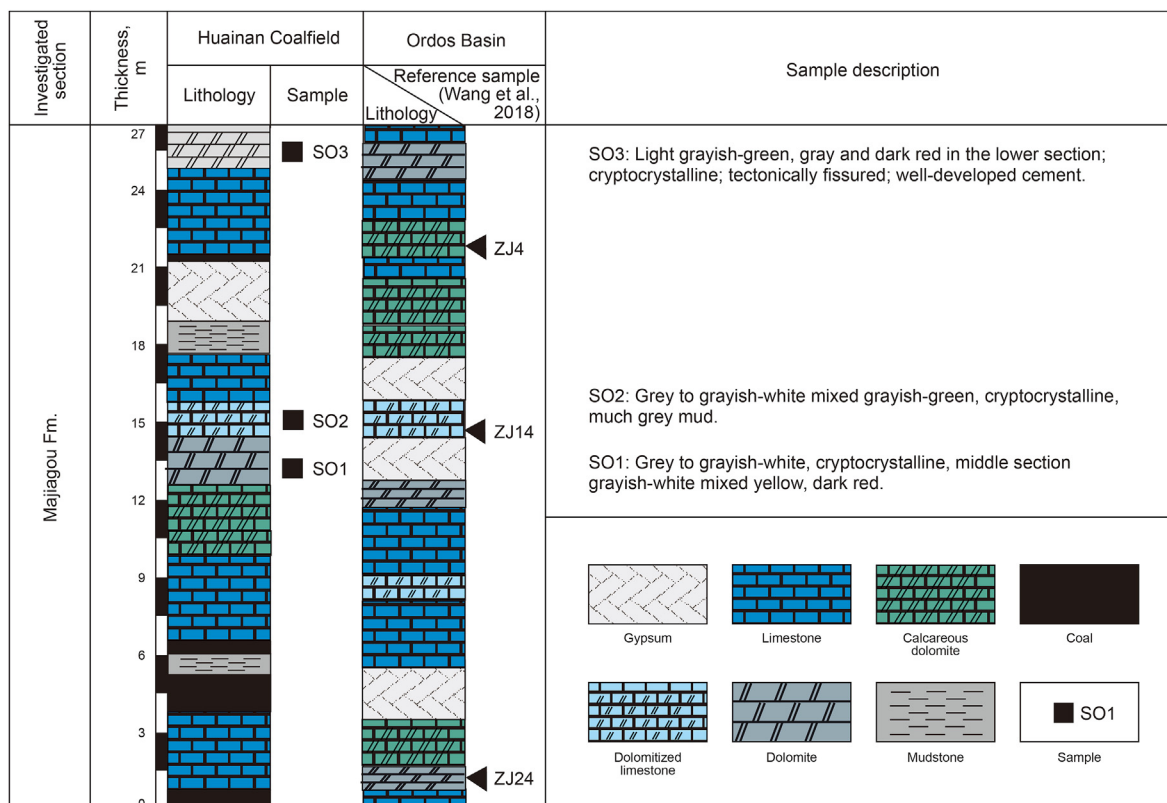


Fig. 2. Schematic stratigraphy of the Majiaogou Formation in the Huainan Coalfield, and comparison with that of the corresponding section in the Ordos Basin (the latter section modified from Wang et al., 2018).

samples from weathering. The selected parts of the samples were ground and sent immediately after preparation to the laboratory of the University of Science and Technology of China.

The samples for investigation in the laboratory were taken from fresh (unweathered) parts of the collected material. These samples were divided into two portions, one for analysis and one as a standby (Fig. 3). The samples for analysis were sliced and ground again according to the specifics of the test. The cutting, carried out with a PetroThin thin-section cutter, yielded slices of 100–150 μm thick. Subsequently, they were ground to 30 μm on a Lapping plate and polished.

The other selected material was crushed with a grinder to less than 60-mesh and subsequently ground in an agate mortar with a grinding rod to 160–200-mesh. This ground material was divided into four portions of approx. 100 g each, which were stored in numbered brown glass bottles.

The chosen samples were analyzed for major elements, trace elements, REE, and C and O isotopes. The weight of each sample used for a specific laboratory test was at least 50 mg (Fig. 3).

3.2. Analyses

The selected samples were investigated in order to identify the constituting minerals (see 3.2.1), to determine the concentrations (as oxides) of the major elements (3.2.2), to determine the contents of trace elements (including REE) (3.2.3), and to establish the ratios of the stable carbon and oxygen isotopes (3.2.4).

3.2.1. Microscopic identification

The original core samples were sliced, gold plated, and identified under a DM4P polarizing microscope and a KYKY2800B scanning electron microscope (SEM), respectively. Representative parts were photographed for further analysis.

3.2.2. Analysis of major oxides

At least 10 g of each sample was taken for X-ray fluorescence (XRF) analysis of the major elements. The powdered samples were calcined at 70 °C for 12 h. The CaO, MgO, MnO, and Fe₂O₃ contents were determined with an Axiosm AX fluorescence spectrometer. The range of this element analysis was from Be (4) to U (92). The

reproducibility of the goniometer was 0.0001°.

3.2.3. Analysis of trace elements and rare earth elements

The main trace elements and REE (Sr, Ba, Ga, La, Ce, and Pr) were measured with a NexION 300D inductively coupled plasma mass spectrometer (ICP-MS). The powder was crushed to 200 mesh (fine samples are easily dissolved by acetic acid leachates). The peak value jumped one point per mass. The cooling air-flow rate was 5 L per minute, and the sample lift rate was 1 mL per minute. The measurement standards were GSS-5, GSR-6, GSD-12, and DZ-1 (see Zhu et al., 2010), and the measurement error was less than 5%.

3.2.4. ¹³C and ¹⁸O isotope analysis

The ¹³C and ¹⁸O isotopes were measured from whole-rock powder. The powder was crushed to >200 mesh and dissolved in HCl. Subsequently, it was heated at a constant temperature of 850 °C. A Mat-252 isotope mass spectrometer with 1000 mol/ion sensitivity was used. The vacuum degree of the ion source was <30 × 10⁻⁹ mbar; the analysis chamber vacuum degree was <50 × 10⁻⁹ mbar; the 90° sector magnetic field had a magnetic resonance of 230 mm; the standard deviations of the isotope mass spectrometer were 0.07‰ and 0.04‰ (cf. Valley et al., 1995). All analytical results are indicated according to the Pee Dee Belemnite (PDB) standard.

4. Results

The results are presented following the structure in Section 3.

4.1. General characteristics of the samples

The three samples show characteristics that are described and interpreted here shortly, because this interpretation helps understand the findings regarding the major oxides and trace elements (Section 4.2), and the stable carbon and oxygen isotopes (Section 4.3).

4.1.1. Sample SO1

This dolomite sample shows fissures in thin section (Fig. 4), filled mainly with calcite. At the contact between the fissures and

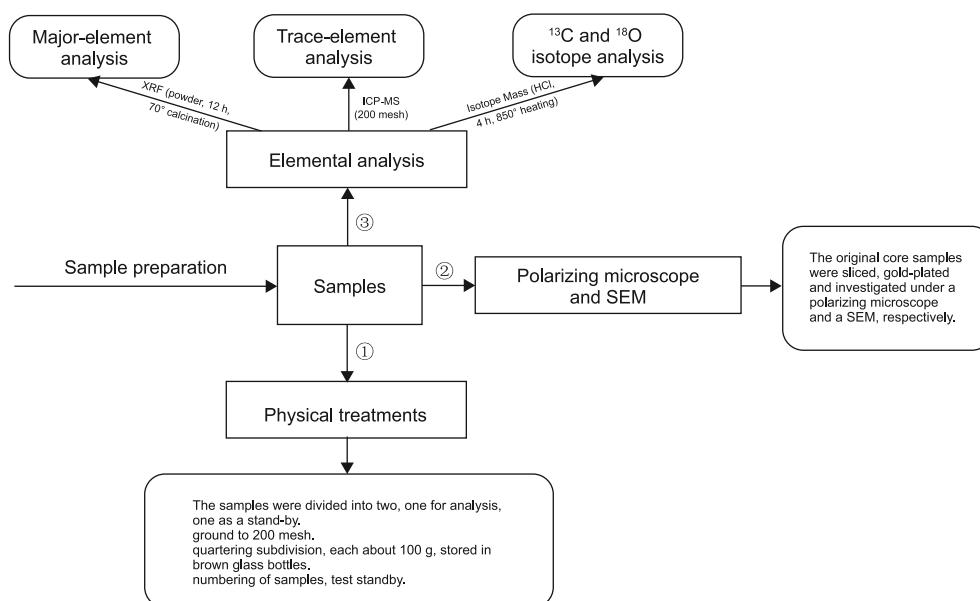


Fig. 3. Flow chart of the sample handling. The numbers indicate the order of handling procedures.

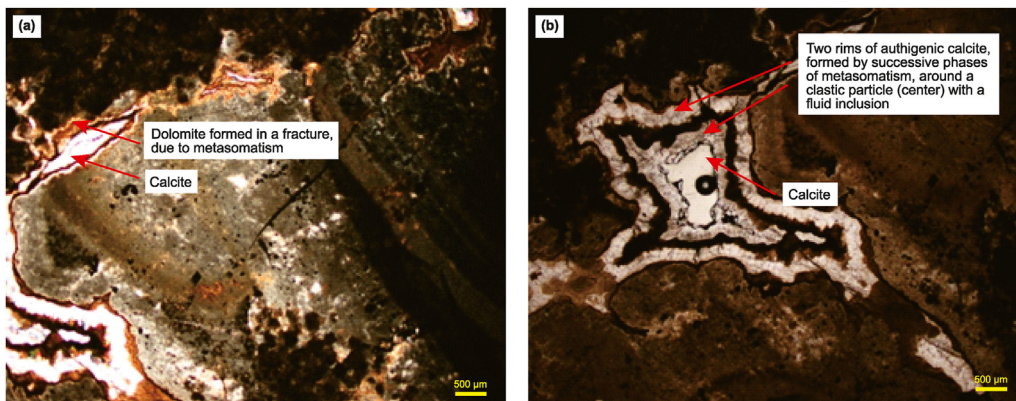


Fig. 4. Thin sections (crossed nicols) of sample SO1, a dolomite. (a): Margin of a fracture caused by the pressure of a metasomatic fluid. (b): Clastic calcite particle with a fluid inclusion (center), surrounded by two metasomatism-induced rims of authigenic calcite, indicating two separate phases of authigenesis.

the micrite matrix, small dolomite particles are locally present attached to the wall. Some grayish argillaceous dolomite was converted into sand-to silt-sized particles (Fig. 4).

The dolomite must have formed from calcite at the edge of the fissure due to dolomitization (Fig. 4a). The transformation of the grayish argillaceous dolomite into sand-to silt-sized particles was due to metasomatism. This process played an important role and resulted also, for instance, in the crystallization of an authigenic calcite rim around a clastic calcite particle (Fig. 4b). After some time, the growth of this rim stopped, but a new growth phase started subsequently so that a second calcite rim developed (Fig. 4b).

4.1.2. Sample SO2

This dolomitic limestone shows less interesting features. The sample consists of calcite grains (Fig. 5a–b) and of micritic limestone with grains of roughly similar sizes, and a small amount of sparry calcite.

4.1.3. Sample SO3

This calcareous dolomite shows a dual character in thin section: one part consists of micrite with a uniform grain size with a few well-developed calcite crystals (Fig. 6), whereas the other part consists of angular to subangular poorly-sorted particles, that clearly show dolomitization, intersected locally by fissures (Fig. 6a), but such fissures are elsewhere absent (Fig. 6b).

The small grain size indicates a low-energy depositional

environment. The particles are detrital and must have been deposited not far away from the source rocks. Because the particles are not in contact with each other, the substrate must have provided sufficient material to cause extensive carbonate cementation. It seems that low-energy currents or waves broke up the semi-consolidated debris in the basin and subsequently buried them, which resulted eventually in compaction. Taken all data together, it must be deduced that the rocks from which sample SO3 was taken represent low-energy subaqueous conditions.

4.2. Major oxides and trace elements

The concentrations of the major elements (as oxides) are presented in Table 1. The major elements in carbonates reflect the influence of the source material and the salinity of the depositional environment; Table 2 shows the concentrations of the relevant trace elements, which reflect diagenesis, alteration degree and depositional environment; the REE concentrations in the three samples (standardized for chondrites) and their main parameters are presented in Table 3 and Table 4. They reflect the redox environment (Eh) at the time of deposition.

In order to increase the insight into the depositional environment of the Majiagou Formation under the Huainan Coalfield, the geochemical data of the Majiagou samples are compared in the following sections with the same data obtained by Wang et al. (2018) for the reference samples of the Majiagou Formation (Fig. 7) in the eastern part of the Ordos Basin (Fig. 2).

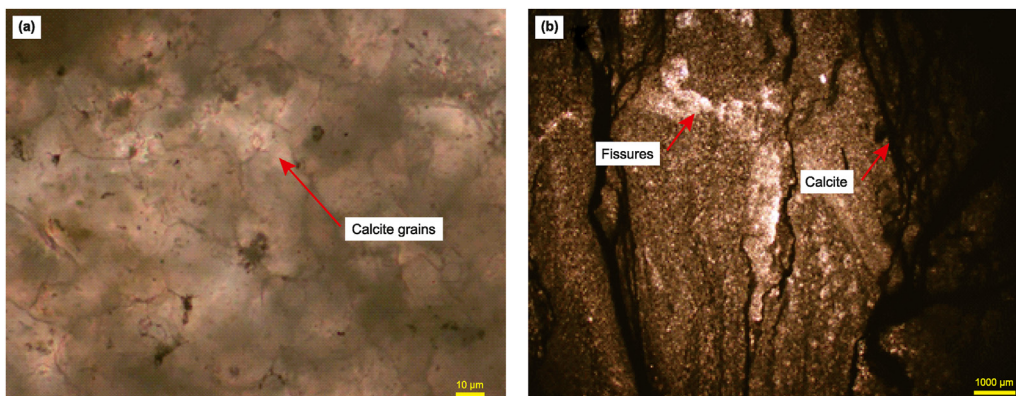


Fig. 5. SEM photographs of sample SO2, a dolomitic limestone. (a): Characteristic texture of calcite grains. (b): Fissures within mostly dolomitic material embedded between calcite.

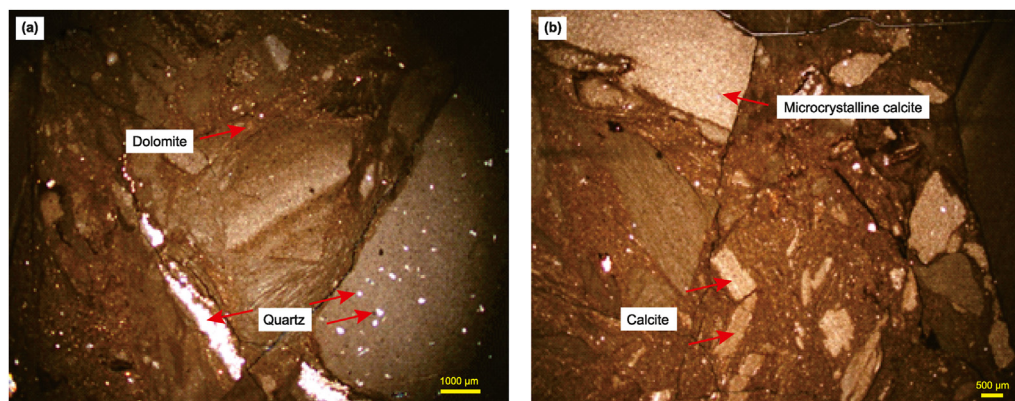


Fig. 6. SEM photographs of sample SO3, a calcareous dolomite. (a): Characteristic texture of dolomite grains. (b): Microcrystalline calcite.

Table 1
Average concentration (in %) of the major elements (as oxides in the three investigated samples).

Sample	Fe ₂ O ₃	MnO	TiO ₂	CaO	K ₂ O	SO ₃	P ₂ O ₅	SiO ₂	Al ₂ O ₃	Na ₂ O	MgO	CaO/MgO	Rock type
SO3	1.480	0.024	0.200	24.430	2.170	0.900	0.060	19.400	4.400	0.010	13.370	1.830	Calcareous dolomite
SO2	0.220	0.004	0.100	45.050	0.930	0.300	0.039	10.320	2.100	0.00	1.660	27.140	Dolomitic limestone
SO1	0.370	0.019	0.000	28.800	0.160	0.100	0.025	9.170	0.200	0.00	19.270	1.490	Dolomite

Table 2
Concentration (in ppm) of the most relevant trace elements of the three investigated samples.

Sample	Sr	Ba	Ga
SO3	72.31	2.37	0.78
SO2	111.72	6.73	3.36
SO1	42.62	14.07	12.32

4.3. ¹³C and ¹⁸O isotopes

The amounts of the stable isotopes of C and O are important proxies for the diagenetic development of carbonate rocks. Table 5 presents the isotopic values of C and O in the three samples. The analyses show that the ¹³C isotope content of the Majiagou samples fluctuates only slightly, from −4.91‰ to +1.24‰. The ¹⁸O isotope content is low and shows medium negative values, ranging from −8.18‰ to −6.78‰.

5. Discussion

Several aspects need more discussion if the conclusions based

Table 3
Standardized values (in ppm) of rare earth elements in dolomite.

Sample	La	Ce	Pr	Nd	Sm	Eu	Gd	Tb	Dy	Ho	Er	Tm	Yb	Lu
SO3	59.03	12.38	30.33	26.33	14.00	9.39	14.05	11.80	3.01	5.57	7.24	5.25	6.12	7.14
SO2	34.19	28.47	17.05	14.52	7.54	4.90	5.21	6.33	3.66	3.34	4.14	3.09	3.83	6.21
SO1	12.68	12.13	7.30	6.55	3.69	2.04	2.47	3.16	1.89	1.53	1.90	1.23	1.39	0.93

Table 4
Main parameters of the rare earth elements in the three investigated samples.

Sample	∑REE (10 ⁻⁶)	LREE (10 ⁻⁶)	HREE (10 ⁻⁶)	L/H ratio	δCe	δEu	(La/Yb) _N	(La/Sm) _N
SO3	211.64	151.46	60.18	2.52	0.29	0.67	9.65	4.22
SO2	142.48	106.67	35.81	2.98	1.18	0.78	8.93	6.97
SO1	58.89	44.39	14.50	3.06	1.26	0.68	9.12	3.44

on the characteristics of the Majiagou Fm. in the study area are to be understood sufficiently well to help exploration for gas (and possibly oil) become more effective. The main aspects to be discussed, on the basis of the data presented in the Results section, regard the depositional environment (5.1), the salinity of the environment (5.2), its redox conditions (5.3), the stable carbon and oxygen isotopes (5.4), the diagenetic history (5.5) and the resulting alteration of the carbonates (5.6).

5.1. Alteration of the carbonates

Particularly the Mg/Ca, Sr/Ca and Mn/Sr ratios provide much information about the alteration of the carbonates of the Majiagou Fm. in the Huainan Basin.

5.1.1. The Mg/Ca and Sr/Ca ratios

Alteration can cause redistribution of trace elements in marine carbonate rocks, particularly due to the percolation of (fresh) meteoric water. The latter contains, in contrast to seawater, only very small amounts of Sr, which implies that the rocks become depleted in Sr. Also Mg is sensitive to such alteration, but Ca is not. If the Mg/Ca ratio consequently changes significantly (by a factor of 2

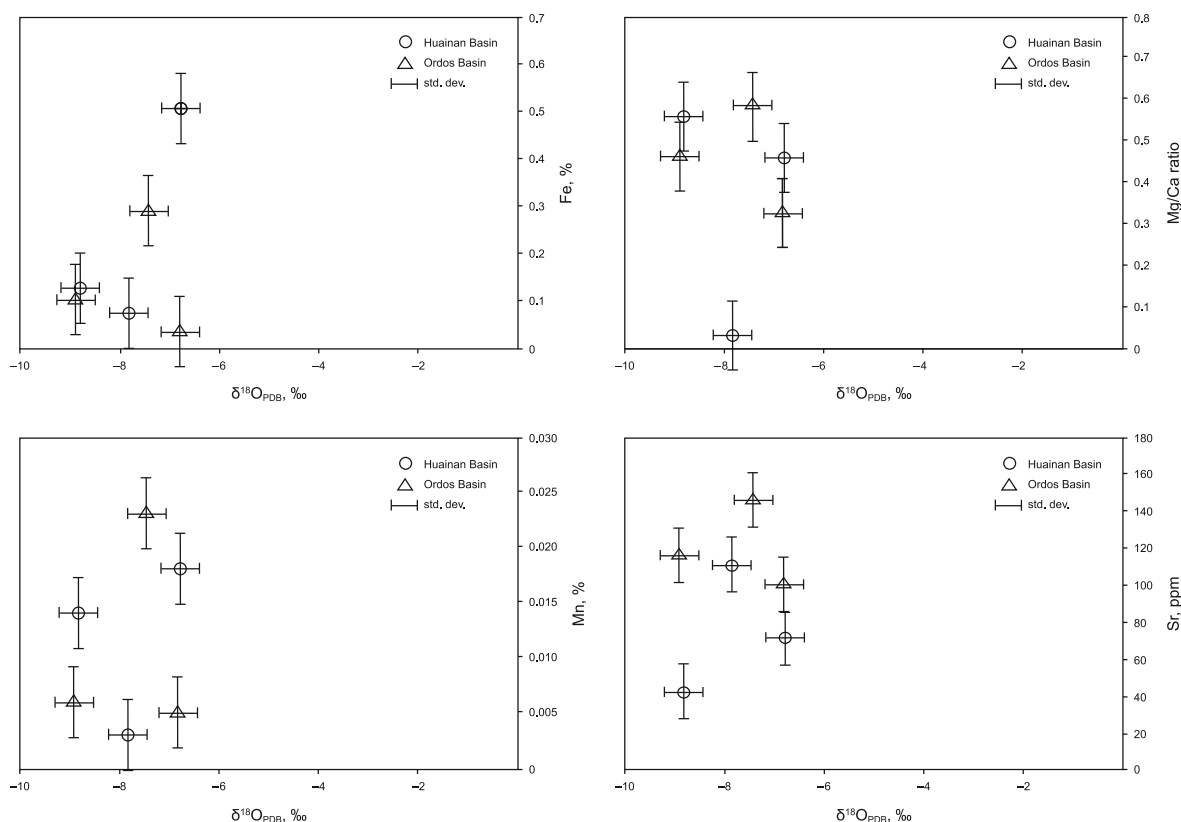


Fig. 7. Oxygen-isotope anomalies in the carbonates under study and in the reference samples (Wang et al., 2013, 2018).

Table 5

Relative values (in ‰) of the stable carbon and oxygen isotopes in the three investigated samples.

Sample	SO3	SO2	SO1
δ ¹³ C	-4.91	-1.16	-1.24
δ ¹⁸ O	-6.78	-7.83	-8.18

or more), the Sr/Ca ratio consequently also decreases significantly. Such a decrease therefore suggests that the carbonates have suffered from strong (commonly late) alteration (Averyt et al., 2003; Bayon et al., 2007; Tian, 2016). Our analyses show (Tables 2 and 6) that the Sr concentration in samples SO1 through SO3 did not diminish that much. The Mg/Ca ratio in sample SO2 was reduced, indeed, but less than in samples SO1 and SO3. This indicates that not the entire Majiagou Formation experienced intense alteration.

The Mg/Ca ratio in sample SO2 is relatively low. This may well have been caused by a relatively large influx of meteoric water into the limestone shortly after deposition. This is not unlikely because of the shallow-marine setting of the lower part of the Majiagou Formation. The Sr/Ca ratios in the investigated samples are 0.0021 (SO1), 0.0035 (SO2) and 0.0414 (SO3) (Table 6). The high values in samples SO2 and SO3 indicate that the lower part of the succession was much more than the upper part exposed to continental

Table 6

Mn/Sr, Mg/Ca, Sr/Ca ratios in the three investigated samples.

Sample	SO3	SO2	SO1
Mn/Sr	0.41	0.12	0.58
Sr/Ca	0.0414	0.0034	0.0021
Mg/Ca	0.459	0.031	0.562

conditions that allowed the precipitation of rainwater.

5.1.2. The Mn/Sr ratio

The Mn/Sr ratio is a sensitive proxy for judging the diagenesis and alteration degree of marine carbonates. The higher the content of Sr and the lower the content of Mn, the lower the Mn/Sr ratio will be. Because a high Sr content indicates little influence of rain water (see the above section), this implies that a low Mn/Sr ratio indicates reliable information about the characteristics of the seawater during deposition of the carbonates (cf. Derry et al., 1989; Kim et al., 1999). An Mn/Sr ratio <2 is commonly considered to represent weak or non-existent diagenetic alteration (e.g. Jacobsen and Kaufman, 1999; Korte et al., 2003, 2006; Huang, 2010).

The Mn/Sr ratios of our samples range from 0.41 to 0.58, and thus all are less than 1. It is therefore likely that the carbonates under study were not diagenetically altered.

5.2. Sedimentary environment

The interpretation of the sedimentary environment of a specific geological unit is commonly based primarily on field observations regarding lithology, facies and lateral and vertical facies shifts, fossil content, sedimentary structures, etc. Such data are absent here, however, because only some cored sections (from which 3 samples were taken) are available. Consequently, most data that can help reconstruct the sedimentary environment must be derived from the samples. These were investigated for their chemical composition on the basis of the content of both the major elements (as oxides) (5.1.1) and the trace elements (5.1.2).

5.2.1. Sedimentary environment as deduced from the major elements

Clay minerals adsorb K and Na that is present in the water in the sedimentary environment where clay minerals are deposited (Gerdes et al., 2002). The higher the water salinity, the more K and Na are adsorbed, but K is more easily adsorbed than Na. The content of $K_2O + Na_2O$ in carbonate rocks can therefore be used as a proxy for the salinity of the depositional environment. The lower the Na_2O/K_2O ratio, the higher the salinity of the water was.

In the samples under study here, the total amount of

$K_2O + Na_2O$ was largest in sample SO3 (the calcareous dolomite), while its Na_2O/K_2O ratio was close to the minimum (Table 1, Fig. 8a). This implies that the salinity of the sea water was high. As will be detailed in the section about the trace-element analysis (5.1.2), the climatic was hot and humid, so that it may be presumed that the evaporation was strong, which unavoidably increased the salinity of the seawater.

Remarkably, the Na_2O concentration in the reference samples ZJ4, ZJ14 and ZJ24 (Wang et al., 2018) is higher than in the samples from the Huainan Basin under study, where this value tends to be

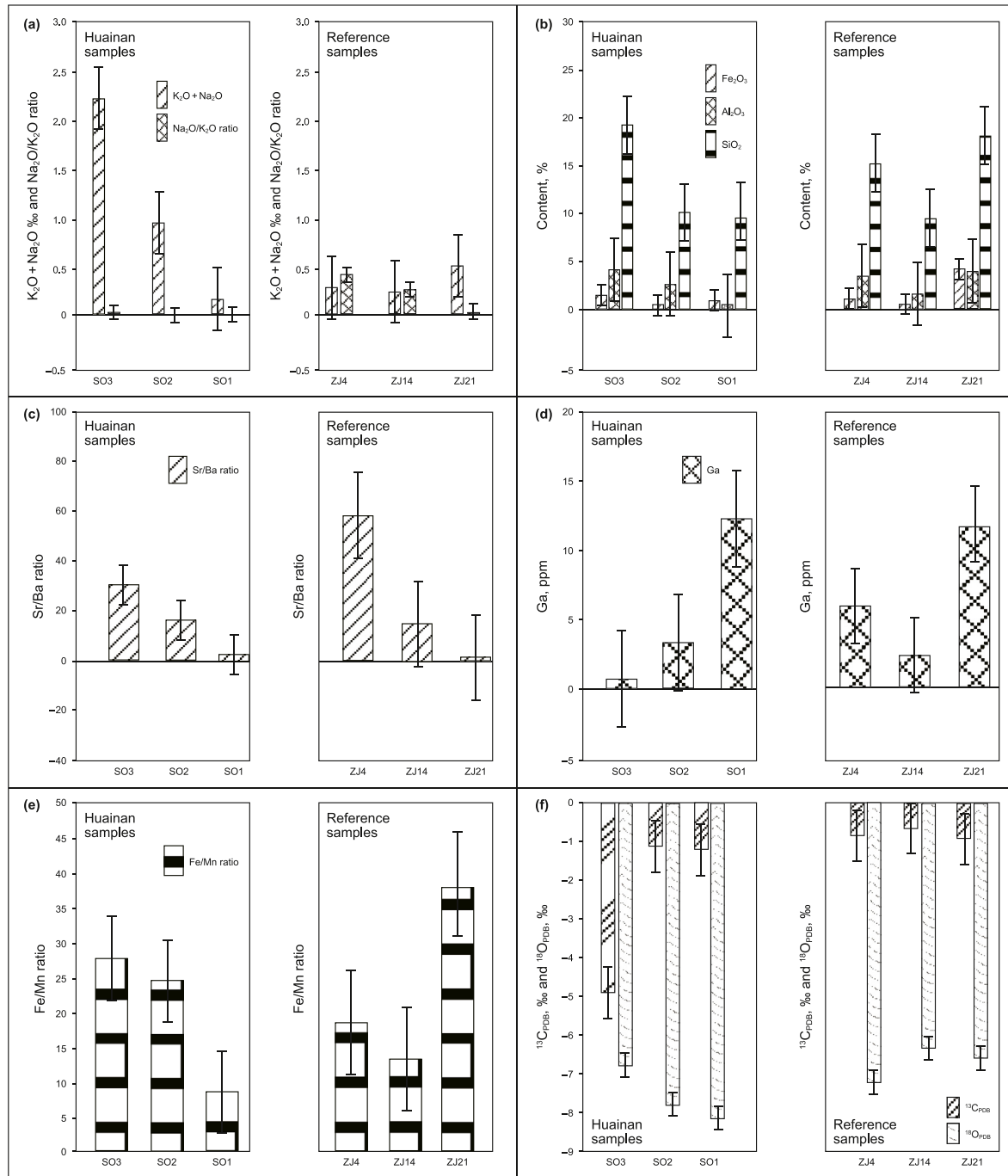


Fig. 8. Comparison of the characteristics of the major elements in the carbonates of the Majiagou Formation under the Huainan Coalfield (left) and in the eastern Ordos Basin (right) (Wang et al., 2013, 2018). (a): Relationship between the K_2O and Na_2O content. (b): Relationships between the Fe_2O_3 , Al_2O_3 and SiO_2 content. (c): Sr/Ba ratios in the carbonates. (d): Ga concentrations. (e): Fe/Mn ratios. (f): Carbon and oxygen isotope anomalies.

practically nil. This is because Na ions occupy crystal defects in the carbonate crystals that resulted in voids in the crystal lattice (cf. Morse and Mackenzie, 1990). There must have been many such spaces in the carbonates' lattices, while the Na content in the shallow-marine carbonates was high. The number of crystal defects decreased, however, with ongoing burial diagenesis, so that the defect-related spaces in the lattice decreased, and the carbonates consequently lost Na continuously (cf. Malone et al., 2001).

The deep burial that the Majiagou Formation underwent in the Huainan area (and that led to the loss of Na) is due to the tectonic context. Since the Middle Ordovician, the North China Block was uplifted as a consequence of the subduction of plates at both sides; this uplift resulted, obviously, in denudation. This changed in the Late Carboniferous, when the southern part of the North China Block was converted into a subsiding basin (Chen, 2000; Meng et al., 2018), eventually leading to deep burial of the Majiagou Formation.

The supply of terrigenous material had a significant impact on the depositional conditions of the carbonates. The sediments became enriched in components that were resistant to weathering, such as SiO₂, whereas some elements that were easily set free because of weathering or because they went easily into solution, such as Fe and Al, precipitated when the pH of the seawater changed. The enrichment of these elements (in the form of variations in the contents of the Fe, Al and Si oxides) in the investigated samples (Fig. 8b) shows the significant influence of the terrigenous input (cf. Pattan et al., 2005; Acharya et al., 2015; Yu et al., 2017). The amounts of SiO₂ and Al₂O₃ increased gradually from SO1 to SO3. This indicates that the input of terrigenous material gradually increased, and thus that the weathering and denudation of the source area became stronger. The SiO₂ content of Majiagou Formation in the reference samples from the Ordos Basin (Wang et al., 2018) is lower than in the Huainan Basin, which is strong evidence that the Huainan Basin was situated more closely to the source area of the terrigenous material than most of the rest of the Ordos Basin.

5.2.2. Trace-element analysis

The distribution of trace elements in sediments (or sedimentary rocks) is determined not only by the sedimentary environment and the geochemical properties of the elements themselves, but is also influenced by alteration and other diagenetic processes (Pruysers et al., 1991; Zhou et al., 2000; Abanda and Hannigan, 2006; Wang and Sun, 2013; Gong et al., 2018). Consequently, the concentrations of the various trace elements can provide information about the depositional conditions only if diagenesis did not or hardly affect the sediments. On the other hand, the concentrations of trace elements can be used to analyze the diagenetic processes and the degree of diagenesis.

The trace elements in the samples under study were found to provide information about both the depositional conditions (e.g. salinity of the seawater; see Section 5.2) and the diagenetic alterations (see Section 5.6).

5.3. Salinity

It has been found in numerous studies that some trace elements can provide information about the salinity of the water in which sediments accumulated. This holds particularly for the Sr/Ba ratio (e.g., Wei and Algeo, 2020; Wang et al., 2021) and the gadolinium (Ga) content (e.g., Zhu et al., 2004; Paffrath et al., 2020).

5.3.1. The Sr/Ba ratio

The Sr/Ba ratio is often analyzed with the purpose to reconstruct the salinity of the depositional aquatic environment of both marine and continental sediments. The chemical properties of Sr and Ba are

similar, but their ratios are influenced by the sedimentary environment because of differences in geochemical behavior (Adegoke et al., 2014; Paytan et al., 2007; Stüeken et al., 2020; Wei and Algeo, 2020; Wang et al., 2021): Sr has stronger migration ability than Ba so that, when the salinity of the water increases gradually due to evaporation, precipitation in the form of BaSO₄ occurs first. When the lake or sea water is concentrated to a certain extent, SrSO₄ can precipitate. Thus, Sr and Ba compete for sulfate ions, which leads to reverse growth and decline in their content. Consequently, the content of Sr or – better – the Sr/Ba ratio can be used as a proxy for the salinity during sedimentation (Liu et al., 1993; Gerdes et al., 2002; Yang et al., 2017).

The extracted Sr/Ba ratios are <1.0 in fresh (fluvial) water, 1.0–3.0 in brackish water (delta front), 3.0–8.0 in saltwater (pro-delta), and >8.0 in normal seawater (neritic environments) (Wang et al., 2021). The range of the Sr/Ba ratio in the samples from the Majiagou Formation is 3.03–30.51 (Fig. 8c). Only the Sr/Ba ratio of sample SO1 is higher than 3 and lower than 8. These values for samples SO2 and SO3 are much higher than 8. This shows that the carbonates under study were minimally affected by influx of fresh water from a continent, so the depositional environment was truly marine. A similar conclusion has been drawn by Wang et al. (2018) for the three reference samples from the Majiagou Formation.

5.3.2. Ga content

Also the Ga content in carbonate sediments can be used for distinguishing marine from continental deposits (Sahlström et al., 2017): if the Ga concentration is less than 15 ppm, it indicates marine conditions, whereas a range between roughly 18 and 23 ppm indicates continental deposition (Landsberger and Bode, 1990; Feng, 2000; Sahlström et al., 2017; Yang et al., 2017).

The concentration of Ga in the samples under study varies from 0.78 to 12.32 ppm (see Table 2), and is consequently less than the value of 15 ppm which is commonly taken as the boundary value between a marine and a fresh-water environment. This indicates a marine depositional environment. Similar findings have been obtained for the three reference samples from the Majiagou Formation (Fig. 8d).

5.3.3. Conclusions regarding the salinity

By combining the above data concerning the Sr/Ba ratio and the Ga concentrations in both our samples and the reference samples described by Wang et al. (2018), it must be deduced that the sedimentary environment of the Majiagou Formation in the Huainan Basin was, regarding the salinity of the water, well comparable with that of the Ordos Basin in the area studied by Wang et al. (2018): normal marine conditions prevailed.

5.4. Redox conditions

Rare earth elements (REE) are commonly used for the reconstruction of the depositional environment because of their unique geochemical behavior and their sensitivity to environmental changes. Negative values of δCe and δEu indicate a reducing environment (Elderfield and Pagett, 1986; Wright et al., 1987; McLennan, 1989, 2018; Webb and Kamber, 2000; Ounis et al., 2008; Himmler et al., 2010; Li et al., 2017; Caetano-Filho et al., 2018). The REE content in carbonate rocks has been standardized for chondrites (the standardization of values is indicated by the subscript letter N, e.g. Ce_N; Ce_N thus represents the value of Ce presented on the basis of the laboratory analysis divided through the standardized Ce value).

The REE values in the investigated samples show a poor correlation between δCe and La_N/Sm_N (Fig. 9a), indicating that the Ce concentration represents the concentration in the original

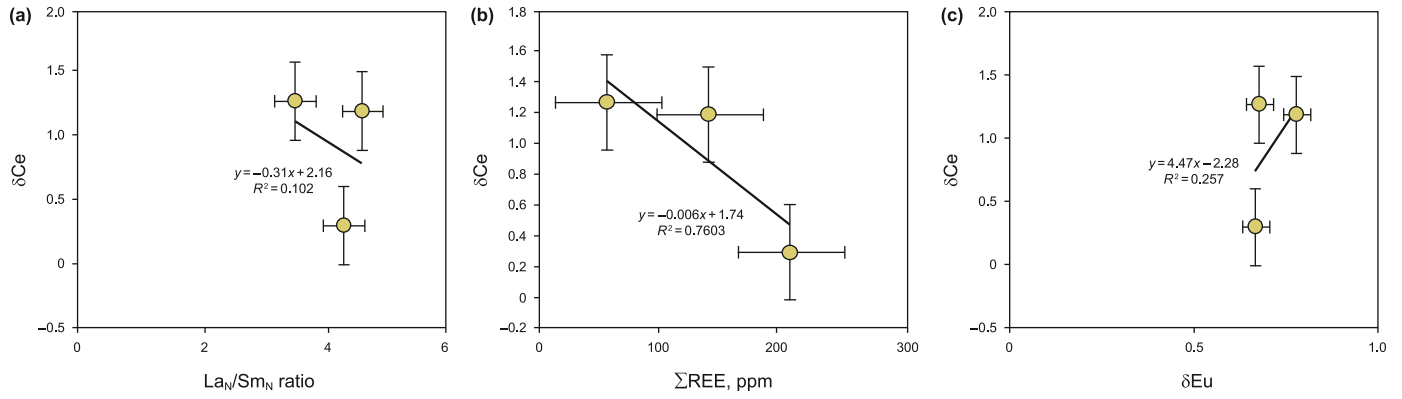


Fig. 9. Characteristic scatter plots of rare earth elements and trace elements in carbonate rocks from the Majiagou Formation in the Ordos Basin (Qiang et al., 2015).

sediment and that it was hardly affected by diagenesis or weathering. The weak correlation between δCe and the sum of all REE (ΣREE) in the three samples (Fig. 9b) indicates that diagenesis had only a limited influence on the negative Ce anomalies in the REE, and the same holds for the correlation between δEu and ΣREE (Fig. 9c), which supports this conclusion. Fig. 10 shows the normalized distribution pattern of the REE.

The cerium anomaly (Ce/Ce^* or δCe) can also be calculated by $\delta\text{Ce} = \text{Ce}_N/(\text{La}_N \cdot \text{Pr}_N)^{1/2}$, where N is the standard value for chondrites. If $\delta\text{Ce} > 1$, it is considered a positive anomaly, and if $\delta\text{Ce} < 0.95$, it is considered a negative anomaly (Lanzirott and Hanson, 1996; Liang et al., 2005; Huang et al., 2008; Zhang et al., 2011).

The values of δCe in the samples SO1 through SO3 range from 0.29 to 1.26. The δCe value in the SO3 dolomite sample is less than 0.95, indicating a reducing aqueous environment, suggesting that the sea was deep. In our lowermost sample, SO1 (dolomite), and the middle sample, SO2 (dolomitic limestone), the δCe value of >1 indicates an oxidizing water body, suggesting a shallow environment.

Regarding the Eu values, it is known (e.g., Lanzirott and Hanson, 1996; Zhao and Gao, 1998; Liang et al., 2005) that $\delta\text{Eu} = \text{Eu}_N/(\text{Sm}_N \cdot \text{Gd}_N)^{1/2}$. In the samples under study, δEu ranges from 0.67 to 0.78, thus showing only slight anomalies (see Fig. 10 for the normalized distribution pattern of REE). The figure shows that the REE are more abundant on the left side and less on the right side, which indicates LREE enrichment and HREE depletion. In this respect, the samples under study are well comparable to the values

of the reference samples investigated by Wang et al. (2018). Both sample groups also show a negative Eu anomaly, indicating that they were both formed in an alkaline reducing environment (cf. Puchelt and Emmermann, 1976; Huang et al., 2008; Qiang et al., 2015; Xie et al., 2019).

5.5. Stable carbon and oxygen isotopes

The study of stable C and O isotopes in carbonate rocks is widely used for the quantitative interpretation of the salinity and the water temperature during deposition, and for analysis of the diagenetic environment and the resulting alterations (Garcés et al., 1995; Land and Hoops, 1973; Spielhagen and Erlenkeuser, 1994; Gillikin et al., 2006; Baghdady et al., 2017; Nicolas et al., 2018). The values of the C and O isotopes in the carbonates under study here are shown in Table 5.

Fig. 8f shows the $^{13}\text{C}_{\text{PDB}}$ and $^{18}\text{O}_{\text{PDB}}$ values for both the investigated and the reference samples. The ^{13}C and ^{18}O values of all three samples under study here are medium to slightly negative. This is consistent with the environmental requirements for the formation of dolomite and limestone: the dolomite was formed in a shallow, strongly saline marine environment in a hot, arid climate with much evaporation. The light carbon and oxygen isotopes evaporated preferentially so that the heavy isotopes became relatively enriched in the seawater (cf. Spielhagen and Erlenkeuser, 1994).

Keith and Weber (1964) combined ^{13}C and ^{18}O data to estimate the salinity of a depositional environment and to distinguish marine from continental deposits by the so-called Z-value: $Z = 2.048 (\delta^{13}\text{C} + 50) + 0.498 (\delta^{18}\text{O} + 50)$. A Z-value > 120 indicates a marine depositional environment, whereas a value < 120 indicates a continental environment (Z = 120 is not decisive). We found that both the samples SO1 and SO2 have Z-values over 120, thus indicating a marine sedimentary environment, whereas that of SO3 is less than 120, thus suggesting a fresh-water (possibly brackish) sedimentary environment. This indicates that the Majiagou Formation was initially deposited in a marine environment, but that later, when the climate on the North China Platform had changed to dry and hot, and when the basin was uplifted and the sea level dropped (Chen, 2000; Meng et al., 2018), the influence of atmospheric fresh water increased.

5.6. Diagenetic development

The diagenesis of the carbonates of the Majiagou Formation in North China has been studied particularly for the Ordos Basin (Huo et al., 2014; Wei et al., 2017; Liu et al., 2020; Xiong et al., 2020). Relatively few studies are available for the eastern part of North

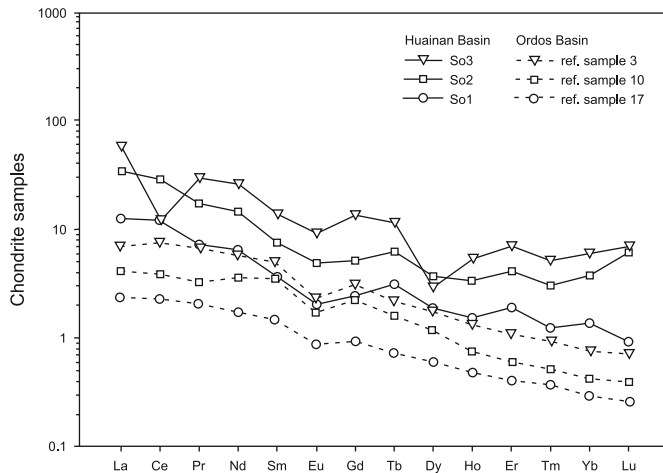


Fig. 10. REE distribution picture in the carbonates under study and in the reference samples (Tian and Xiao, 2013; Wang et al., 2018).

China, except for the region around the city of Langgu (Xiang et al., 2020), where dolomite is dominant in the lower part of the formation, gray micritic limestone dominates the middle part, and the upper part consists again mainly of dolomite. No comparable studies are available for the Huainan Basin.

The three investigated samples (SO1–SO3) show some interesting diagenetic features. Sample SO1 (dolomite) must have been subjected to fluid-induced metasomatism, as evidenced by its abundant pores; the resulting dolomitization is significant. Overall, SO1 underwent strong pressure solution and dolomitization. Sample SO2 (dolomitic limestone) shows distinct pressure solution, as well as cementation of the grains in a mosaic pattern. The pressure solution of the rock caused, in combination with the percolating fluids, that earlier compaction-induced tension joints in sample SO2 became filled with calcite. Although the pressure solution in SO2 is significant, mainly in the gray micrite, its dolomitization is not as significant as that in SO1. It may well be that the dolomitization occurred through leaching in a late stage. Sample SO3 (calcareous dolomite) was also subjected to compaction and diagenesis but to a lesser degree due to the above-mentioned uplift of the basin, which explains its still calcareous composition. This is consistent with the findings of Wang et al. (2018) who also analyzed the reference samples in detail, as well as with other studies (e.g. Fu et al., 2019; Su et al., 2021). Moreover, comparison with previous studies indicates that the diagenesis in the Huainan Basin is well comparable to that in the North China Corridor (Xue, 2018).

Trace elements can be important tools for the reconstruction of the diagenetic development (Kranz, 1976; Horowitz and Cronan, 1976; Pingitore, 1978). Particularly the distribution of Sr, Mn, Fe, and some other elements can be helpful. Atmospheric fresh water can cause depletion in Sr (Chester and Stoner, 1974; Brand, 1980; Lu et al., 2005; Read et al., 2016). Marine carbonates can undergo such a process shortly after deposition, and Fe and Mn may be enriched simultaneously. The three investigated samples show that the carbonates became enriched in Sr and depleted in Mn during early diagenesis, and that dolomitization occurred in a late stage. Strong evidence for late-diagenetic dolomitization is also provided by the relationship between the Ca/Mg ratio and the concentrations of Sr and Mn in the samples (Fig. 11), also for the reference samples (Wang et al., 2018). The Ca/Mg ratio is significantly higher than 1, which indicates that the dolomites of the Majiagou Formation were formed in an environment that was sometimes full-marine, but that there was sometimes a brackish or even fresh-water setting.

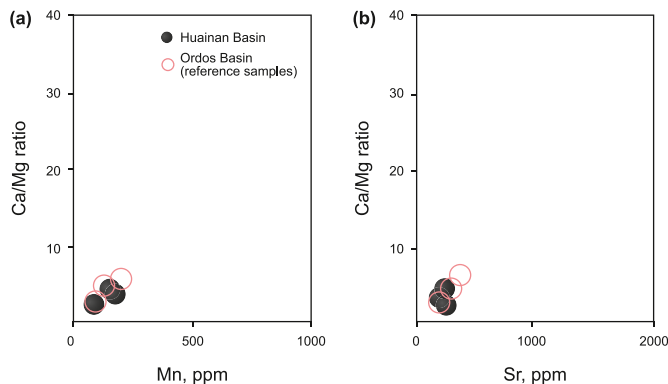


Fig. 11. Relationship between the Ca/Mg ratio and other elements in the carbonates of the Majiagou Formation. (a): Relationship with Mn. (b): Relationship with Sr. Data of the reference samples from Wang et al. (2018).

6. Comparison with the reference samples

In order to increase the effectivity of exploration for gas (and possibly oil) in the deeply buried Majiagou Formation under the Huainan Coalfield, a good insight into the depositional and diagenetic characteristics is required. This has been done by a number of analyses. Comparison with the characteristics of the reference samples (Fig. 7) described by Wang et al. (2018), which are the only samples of the Majiagou Formation investigated thus far in a comparable way, can indicate whether the carbonates under investigation here are comparable with (or different from) the reference samples. The more similarities these two series of samples show, the more likely it is that the rocks under study are comparable with their exposed or shallowly buried equivalents in the eastern part of the Ordos Basin, of which much more is known. This would, obviously, help interpret the possible target areas for hydrocarbon exploration under the Huainan Coalfield.

Because the various geochemical characteristics of the Majiagou Formation in the Huainan Basin have been described and interpreted in the above sections, we will not repeat them here. Rather, we emphasize the comparative results between the geochemical characteristics of the samples from the Huainan Basin with the reference samples of Wang et al. (2018) and with other data from the Ordos Basin.

6.1. Comparison of the sedimentary environment

The main oxides (Fe_2O_3 , Al_2O_3 and Si_2O_3) (Fig. 8) do not show significant differences between our and the reference samples (Fig. 8b). This indicates that the depositional environments at both study sites were comparable. The Sr/Ba ratios also show comparable variations. Because these ratios exceed a value of 1 (Fig. 8c–d), the depositional environment must have been marine.

The Ga concentrations of both series of samples are below 15 ppm, also indicating a marine environment (Pattan et al., 2005; Acharya et al., 2015; Yu et al., 2017; Wang et al., 2018), supporting the above interpretation.

6.2. Comparison of the redox conditions and isotope compositions

The LREE of both series of samples show enrichment, whereas the HREE show depletion (Fig. 10). δEu shows a slightly negative anomaly, indicating a relatively alkaline reducing environment (cf. Wright et al., 1987; Qiang et al., 2015; Li et al., 2017; Caetano-Filho et al., 2018), which is supported by the high Fe/Mn ratios in both series of (Fig. 8e).

The ^{13}C and ^{18}O values in both sample series are medium to slightly negative. The so-called Z-values, calculated following Spielhagen and Erlenkeuser (1994) indicate that the depositional environment was initially normal marine but that the water became later brackish to fresh.

The comparable outcomes of the data concerning both series of samples is understandable, because both study areas are situated on the North China platform which became uplifted, resulting in a falling relative sea level, so that both areas became exposed to fresh water (Baghdady et al., 2017; Nicolas et al., 2018; Wei and Algeou, 2020; Wang et al., 2021).

7. Conclusions

The present study leads to the following main conclusions.

Analysis of the petrology, major elements, and trace element of samples from the carbonates of the Middle Ordovician Majiagou Formation under the Huainan Coalfield indicates that these rocks are basically dolomites (sample SO1 is a dolomite, SO2 is a

dolomitic limestone, and SO₃ is a calcareous dolomite) that formed in a marine environment unaffected by terrigenous input.

The major and trace elements indicate, on the basis of the MgO/CaO, Sr/Ba and Fe/Mn ratios, as well as the Ga content, a humid and hot climate with increased salinity of the marine depositional environment. The low negative values of $\delta^{13}\text{C}$ and $\delta^{18}\text{O}$ indicate that the dolomite was formed in a high-temperature environment after burial. The δEu and δCe values indicate an alkaline, commonly reducing environment.

The geochemical characteristics of the investigated samples from the Majiagou Formation, collected from cores reaching the formation below the Huainan Coalfield, are compared with those from samples collected from the eastern part of the Ordos Basin. The analyses indicate overall well-comparable characteristics of the depositional environment, including salinity and redox conditions.

Considering that the Majiagou Formation in the eastern part of the Ordos Basin contains important oil and gas reservoirs, it must therefore be deduced that it is economically advisable to investigate the Majiagou Formation below the Huainan Coalfield in much more detail, because it is a promising target for hydrocarbon exploration.

Acknowledgements

This work was financially supported by the National Key R&D Plan of China (Grant No. 2017YFC0601405), the National Natural Science Foundation of China (Grant No. 41772096), the Youth Innovation Team Development Plan of Universities in Shandong Province, the Shandong Province Key Research and Development Plan (Grant No. 2019GGX103021) and the SDUST Research Fund (Grant No.2018TDJH101).

References

- Abanda, P.A., Hannigan, R.E., 2006. Effect of diagenesis on trace element partitioning in shales. *Chemical Geology* 230 (1), 42–59. <https://doi.org/10.1016/j.chemgeo.2005.11.011>.
- Acharya, S.S., Panigrahi, M.K., Gupta, A., et al., 2015. Response of trace metal redox proxies in continental shelf environment: the eastern Arabian Sea scenario. *Continental Shelf Research* 106, 70–84. <https://doi.org/10.1016/j.csr.2015.07.008>.
- Adegoke, A.K., Abdullah, W.H., Hakimi, M.H., et al., 2014. Geochemical characterization of Fika Formation in the Chad (Bornu) Basin, northeastern Nigeria: implications for depositional environment and tectonic setting. *Applied Geochemistry* 43, 1–12. <https://doi.org/10.1016/j.apgeochem.2014.01.008>.
- Averynt, K.B., Paytan, A., Li, G., 2003. A precise, high-throughput method for determining Sr/Ca, Sr/Ba, and Ca/Ba ratios in marine barite. *Geochemistry, Geophysics, Geosystems* 4 (4). <https://doi.org/10.1029/2002GC000467>.
- Baghdady, A.R., Howari, F.M., Al-Wakeel, M.L.C.O., 2017. Isotope geochemistry of the Florida phosphate of Four Corners and Hardee County mines, USA: implication for genesis and diagenesis. *Journal for Geochemical Exploration* 181, 99–105. <https://doi.org/10.1016/j.jexplo.2017.07.007>.
- Bayon, G., Pierre, C., Etoubleau, J., et al., 2007. Sr/Ca and Mg/Ca ratios in Niger Delta sediments: implications for authigenic carbonate genesis in cold seep environments. *Marine Geology* 241 (1), 93–109. <https://doi.org/10.1016/j.margeo.2007.03.007>.
- Bao, H.P., Yang, F., Cai, Z.H., et al., 2017. Origin and reservoir characteristics of Ordovician dolostones in the Ordos Basin. *Natural Gas Industry* 37 (1), 32–45 (in Chinese). https://kns.cnki.net/kcms/detail/detail.aspx?dbcode=CJFD&dbname=CJFDLAST2017&filename=TRQG2017010006&uniplatform=NZKPT&v=J9hccaoclFq29yql5gYtQBNDdkwHXyVTJ9EO46G_wOGYMAzY553qcbk6GKf20t.
- Brand, J.V., 1980. Chemical diagenesis of a multicomponent carbonate system 1: trace elements. *Journal of Sedimentary Research* 50 (4), 1219–1236. <https://doi.org/10.1306/212F7BB72B24-11D7-8648000102C1865D>.
- Caetano-Filho, S., Paula-Santos, G.M., Dias-Brito, D., 2018. Carbonate REE + Y signatures from the restricted early marine phase of South Atlantic Ocean (late Aptian – albian): the influence of early anoxic diagenesis on shale-normalized REE + Y patterns of ancient carbonate rocks. *Palaeogeography, Palaeoclimatology, Palaeoecology* 500, 69–83. <https://doi.org/10.1016/j.palaeo.2018.03.028>.
- Chen, B., Liu, G., Wu, D., et al., 2018. The elemental geochemical characteristics of aluminous argillites in the Taiyuan Formation from the Huainan Coalfield. *Coal Geology & Exploration* 46 (3), 21–27 (in Chinese). <https://kns.cnki.net/kcms/detail/detail.aspx?dbcode=CJFD&dbname=CJFD&v=ckJHmD7dcGbtDj9M71kjN98hq5zP4DNs6hWb-OLoKenN1qwrJZ-fWhVcQ6rC0X7>.
- Chen, S.Y., 2000. The basin-range coupling in southern North China block during the Late Palaeozoic to Triassic. *Sedimentary Geology and Tethyan Geology* 20 (3), 34–77 (in Chinese). https://kns.cnki.net/kcms/detail/detail.aspx?dbcode=CJFD&dbname=CJFD2000&filename=TTSD200003006&uniplatform=NZKPT&v=3a9uZnX2efScFlbHyDjZjUmDesMUYB0ko381YvsT152hRdyju2UI_fy5iWe2m-E9.
- Chester, R., Stoner, J.H., 1974. The distribution of Mn, Fe, Cu, Ni, Co, Ga, Cr, V, Ba, Sr, Sn, Zn, and Pb in some soil-sized particulates from the lower troposphere over the world ocean. *Marine Chemistry* 2 (3), 157–188. [https://doi.org/10.1016/03044203\(74\)90013-9](https://doi.org/10.1016/03044203(74)90013-9).
- Chilingar, G.V., 1960. Notes on classification of carbonate rocks on basis of chemical composition. *Journal of Sedimentary Research* 30 (1), 157–158. <https://archives.datapages.com/data/sepm/journals/v01-32/data/030/030001/0157.htm>.
- Derry, L.A., Keto, L.S., Jacobsen, S.B., et al., 1989. Sr isotopic variations in upper proterozoic carbonates from svalbard and east Greenland. *Geochimica et Cosmochimica Acta* 53 (9), 2331–2339. [https://doi.org/10.1016/0016-7037\(89\)90355-4](https://doi.org/10.1016/0016-7037(89)90355-4).
- Elderfield, H., Pagett, R., 1986. Rare earth elements in ichthyoliths: variations with redox conditions and depositional environment. *Science of the Total Environment* 49, 175–197. [https://doi.org/10.1016/0048-9697\(86\)90239-1](https://doi.org/10.1016/0048-9697(86)90239-1).
- Feng, J., 2000. Sequence Stratigraphy and Sedimentology of Yili Basin. China University of Petroleum Press, Dongying, pp. 12–14 (in Chinese).
- Feng, Z., 1993. *Sedimentary Petrology 2*. Petroleum Industry Press, Beijing (in Chinese).
- Fu, S., Zhang, C., Chen, A., et al., 2021. Origin and evolution of dolomite reservoirs in the Ordovician Majiagou Formation, central and eastern Ordos Basin, NW China. In: Yang, R., Van Loon, A.J. (Eds.), *The Ordos Basin - Sedimentological Research for Hydrocarbons Exploration*. Elsevier, Amsterdam, pp. 49–67. <https://doi.org/10.1016/B978-0-323-85264-7.00011-4>.
- Fu, S., Zhang, C., Chen, H., et al., 2019. Characteristics, formation and evolution of pre-salt dolomite reservoirs in the fifth member of the Ordovician Majiagou Formation, mid-east Ordos Basin, NW China. *Petroleum Exploration and Development* 46 (6), 1153–1164. [https://doi.org/10.1016/S1876-3804\(19\)60270-3](https://doi.org/10.1016/S1876-3804(19)60270-3).
- Garcés, B.L.V., Kelts, K., Ito, E., 1995. Oxygen and carbon isotope trends and sedimentological evolution of a meromictic and saline lacustrine system: the Holocene Medicine Lake Basin, North American Great Plains, USA. *Palaeogeography, Palaeoclimatology, Palaeoecology* 117 (3), 253–278. [https://doi.org/10.1016/00310182\(94\)00136-V](https://doi.org/10.1016/00310182(94)00136-V).
- Gerdes, A., Montero, P., Bea, F., et al., 2002. Peraluminous granites frequently with mantle-like isotope compositions: the continental-type Murzinka and Dzhabayk batholiths of the eastern Urals. *International Journal of Earth Sciences* 91 (1), 3–19. <https://doi.org/10.1007/s005310100195>.
- Gillikin, D.P., Lorrain, A., Bouillon, S., et al., 2006. Stable carbon isotopic composition of *Mytilus edulis* shells: relation to metabolism, salinity, $\delta^{13}\text{C}_{\text{DIC}}$ and phytoplankton. *Organic Geochemistry* 37 (10), 1371–1382. <https://doi.org/10.1016/j.orggeochem.2006.03.008>.
- Gong, N., Hong, H., Huff, W.D., et al., 2018. Influences of sedimentary environments and volcanic sources on diagenetic alteration of volcanic tuffs in South China. *Scientific Reports* 8 (1), 7616. <https://doi.org/10.1038/s41598-018-26044-w>.
- Han, Z.Z., Zhang, X.L., Chi, N.J., et al., 2015. Cambrian oncolites and other microbial-related grains on the North China Platform. *Carbonates and Evaporites* 30 (4), 373–386. <https://doi.org/10.1007/s13146-014-0209-2>.
- He, X., Shou, J., Shen, A., et al., 2014. Geochemical characteristics and origin of dolomite: a case study from the middle assemblage of Ordovician Majiagou Formation member 5 of the west of Jingbian gas field, Ordos Basin, north China. *Petroleum Exploration and Development* 41 (3), 417–427. [https://doi.org/10.1016/S18763804\(14\)60048-3](https://doi.org/10.1016/S18763804(14)60048-3).
- Himmeler, T., Bach, W., Bohrmann, G., et al., 2010. Rare earth elements in authigenic methane-seep carbonates as tracers for fluid composition during early diagenesis. *Chemical Geology* 277 (1), 126–136. <https://doi.org/10.1016/j.chemgeo.2010.07.015>.
- Horowitz, A., Cronan, D.S., 1976. The geochemistry of basal sediments from the North Atlantic Ocean. *Marine Geology* 20 (3), 205–228. [https://doi.org/10.1016/00253227\(76\)90116-X](https://doi.org/10.1016/00253227(76)90116-X).
- Huang, S., 2010. *Carbonate Diagenesis*. Geological Publishing House, Beijing, pp. 106–108 (in Chinese).
- Huang, W., Wan, H., Du, G., et al., 2008. Research on element geochemical characteristics of coal-Ge deposit in Shengli Coalfield, Inner Mongolia, China. *Earth Science Frontiers* 15 (4), 56–64. [https://doi.org/10.1016/S1872-5791\(08\)60039-1](https://doi.org/10.1016/S1872-5791(08)60039-1).
- Huo, Y., Pang, Q., Luo, S., et al., 2014. Geochemical characteristics of paleokarst in the Ordovician Majiagou Formation on the southern Jingbian plateau. *Carsologica Sinica* 33 (2), 248–254 (in Chinese). <https://kns.cnki.net/kcms/detail/detail.aspx?dbcode=CJFD&dbname=CJFD2014&filename=ZGYR201402018&uniplatform=NZKPT&v=gqHJp6TC7Oewlj21c5mSGw0APoszcW1x9lyW0cdCW2pglMwbjgY7bP8Ib1RVL>.
- Jacobsen, S.B., Kaufman, A.J., 1999. The Sr, C and O isotopic evolution of Neoproterozoic seawater. *Chemical Geology* 161 (1), 37–57. [https://doi.org/10.1016/S0009-2541\(99\)00080-7](https://doi.org/10.1016/S0009-2541(99)00080-7).
- Keith, A.L., Weber, L.N., 1964. Carbon and oxygen isotopic composition of selected limestone and fossils. *Geochimica et Cosmochimica Acta* 28 (10), 1787–1816.

- [https://doi.org/10.1016/0016-7037\(64\)90022-5](https://doi.org/10.1016/0016-7037(64)90022-5).
- Kim, K.H., Tanaka, T., Nakamura, T., et al., 1999. Palaeoclimatic and chronostratigraphic interpretations from strontium, carbon and oxygen isotopic ratios in molluscan fossils of Quaternary Seoguiipo and Shinyangri Formations, Cheju Island, Korea. *Palaeogeography, Palaeoclimatology, Palaeoecology* 154 (3), 219–235. [https://doi.org/10.1016/S0031-0182\(99\)00112-1](https://doi.org/10.1016/S0031-0182(99)00112-1).
- Korte, C., Jasper, T., Kozur, H.W., et al., 2006. $^{87}\text{Sr}/^{86}\text{Sr}$ record of Permian seawater. *Palaeogeography, Palaeoclimatology, Palaeoecology* 240 (1), 89–107. <https://doi.org/10.1016/j.palaeo.2006.03.047>.
- Korte, C., Kozur, H.W., Bruckschen, P., et al., 2003. Strontium isotope evolution of late permian and triassic seawater. *Geochimica et Cosmochimica Acta* 67 (1), 47–62. [https://doi.org/10.1016/S0016-7037\(02\)01035-9](https://doi.org/10.1016/S0016-7037(02)01035-9).
- Kranz, J.R., 1976. Strontium — ein Fazies-Diagenese-Indikator im Oberen Wettersteinkalk (Mittel-Trias) der Ostalpen. *Geologische Rundschau* 65 (1), 593–615. <https://doi.org/10.1007/BF01808483>.
- Land, L.S., Hoops, G.K., 1973. Sodium in carbonate sediments and rocks; a possible index to the salinity of diagenetic solutions. *Journal of Sedimentary Research* 43 (3), 614–617. <https://doi.org/10.1306/74D7281A-2B21-11D7-8648000102C1865D>.
- Landsberger, S., Bode, P., 1990. Simultaneous determination of gallium and molybdenum in reference materials using epithermal activation analysis and a well-type germanium detector. *Geostandards Newsletter* 14 (1), 149–152. <https://doi.org/10.1111/j.1751-908X.1990.tb00069.x>.
- Lanzirotti, A., Hanson, G.N., 1996. Geochemistry and geochemistry of multiple generations of monazite from the Wepawaug Schist, Connecticut, USA: implications for monazite stability in metamorphic rocks. *Contributions to Mineralogy and Petrology* 125 (4), 332–340. <https://doi.org/10.1007/s004100050226>.
- Li, F., Yan, J., Burne, R.V., et al., 2017. Paleo-seawater REE Compositions and Microbial Signatures Preserved in Laminae of Lower Triassic Ooids. *Palaeogeography, Palaeoclimatology, Palaeoecology*, vol. 486, pp. 96–107. <https://doi.org/10.1016/j.palaeo.2017.04.005>.
- Li, H., Liu, G., Sun, R., et al., 2013. Relationships between trace element abundances and depositional environments of coals from the Zhangji Coal Mine, Anhui Province, China. *Energy Exploration & Exploitation* 31 (1), 89–107. <https://doi.org/10.1260/0144-5987.31.1.89>.
- Liang, T., Zhang, S., Wang, L., et al., 2005. Environmental biogeochemical behaviors of rare earth elements in soil–plant systems. *Environmental Geochemistry and Health* 27 (4), 301–311. <https://doi.org/10.1007/s10653-004-5734-9>.
- Liu, C.Q., Masuda, A., Okada, A., et al., 1993. A geochemical study of loess and desert sand in northern China: implications for continental crust weathering and composition. *Chemical Geology* 106 (3), 359–374. [https://doi.org/10.1016/00092541\(93\)90037-J](https://doi.org/10.1016/00092541(93)90037-J).
- Liu, M., Xiong, Y., Xiong, C., et al., 2020. Evolution of diagenetic system and its controls on the reservoir quality of pre-salt dolostone: the case of the Lower Ordovician Majiagou Formation in the central Ordos Basin, China. *Marine and Petroleum Geology* 122, 104674. <https://doi.org/10.1016/j.marpetgeo.2020.104674>.
- Lu, Z., Ling, H., Zhou, F., et al., 2005. Variation of the Fe/Mn ratio of ferromanganese crusts from the central North Pacific: implication for paleoclimate changes. *Progress in Natural Science* 15 (6), 530–537. <https://doi.org/10.1080/10020070512331342510>.
- Ma, S., 2008. Analysis on Lithofacies Palaeogeography of the Key Sequences of Stratigraphy in Southern North China. Master Thesis. Shandong University of Science and Technology.
- Malone, M.J., Slowey, N.C., Henderson, G.M., 2001. Early diagenesis of shallow-water periplatform carbonate sediments, leeward margin, great bahama bank (ocean drilling program leg 166). *GSA Bulletin* 113 (7), 881–894. [https://doi.org/10.1130/00167606\(2001\)113<0881:EDOSWP>2.0.CO;2](https://doi.org/10.1130/00167606(2001)113<0881:EDOSWP>2.0.CO;2).
- McLennan, S.M., 1989. Rare earth elements in sedimentary rocks; influence of provenance and sedimentary processes. *Reviews in Mineralogy and Geochemistry* 21 (1), 169–200. <https://doi.org/10.1515/9781501509032-010>.
- McLennan, S.M., 2018. Chapter 7. Rare earth elements in sedimentary rocks: influence of provenance and sedimentary processes. In: Lipin, B.R., McKay, G.A. (Eds.), *Geochemistry and Mineralogy of Rare Earth Elements*. De Gruyter, Berlin, pp. 169–200. <https://doi.org/10.1515/9781501509032-010>.
- Meng, Q.R., Wu, G.L., Fan, L.G., et al., 2018. Tectonic evolution of early Mesozoic sedimentary basins in the North China block. *Earth-Science Reviews* 190, 416–438. <https://doi.org/10.1016/j.earscirev.2018.12.003>.
- Meng, X., Ge, M., Tucker, M.E., 1997. Sequence stratigraphy, sea-level changes and depositional systems in the Cambro-Ordovician of the North China carbonate platform. *Sedimentary Geology* 114 (1), 189–222. [https://doi.org/10.1016/S00370738\(97\)00073-0](https://doi.org/10.1016/S00370738(97)00073-0).
- Morse, J.W., Mackenzie, F.T., 1990. *Geochemistry of Sedimentary Carbonates. Developments in Sedimentology*. Elsevier, Amsterdam.
- Munir, M.A.M., Liu, G., Yousaf, B., et al., 2018. Enrichment of Bi-Be-Mo-Cd-Pb-Nb-Ga, REEs and Y in the permian coals of the huainan coalfield, anhui, China. *Ore Geology Reviews* 95, 431–455. <https://doi.org/10.1016/j.oregeorev.2018.02.037>.
- Nicolas, C., Sven, M., Edgar, K., et al., 2018. Palaeoenvironmental and diagenetic reconstruction of a closed-lacustrine carbonate system – the challenging marginal setting of the Miocene Ries Crater Lake (Germany). *Sedimentology* 65 (1), 235–262. <https://doi.org/10.1111/sed.12401>.
- Ounis, A., Kocsis, L., Chaabani, F., et al., 2008. Rare earth elements and stable isotope geochemistry ($\delta^{13}\text{C}$ and $\delta^{18}\text{O}$) of phosphorite deposits in the Gafsa Basin, Tunisia. *Palaeogeography, Palaeoclimatology, Palaeoecology* 268 (1), 1–18. <https://doi.org/10.1016/j.palaeo.2008.07.005>.
- Paffrath, R., Pahnke, K., Behrens, M.K., et al., 2020. Rare earth element behavior in a sandy subterranean estuary of the southern North Sea. *Frontiers in Marine Science* 7, 424. <https://doi.org/10.3389/fmars.2020.00424>.
- Pattan, J.N., Masuzawa, T., Borole, D.V., et al., 2005. Biological productivity, terrigenous influence and noncrustal elements supply to the Central Indian Ocean Basin: paleoceanography during the past ~ 1 Ma. *Journal of Earth System Science* 114 (1), 63–74. <https://doi.org/10.1007/BF02702009>.
- Paytan, A., Avery, K., Faul, K., et al., 2007. Barite accumulation, ocean productivity, and Sr/Ba in barite across the paleocene–eocene thermal maximum. *Geology* 35 (12), 1139–1142. <https://doi.org/10.1130/G24162A.1>.
- Pingitore, N., 1978. The behavior of Zn^{2+} and Mn^{2+} during carbonate diagenesis. *Theory and applications Journal of Sedimentary Research* 48, 799–814. <https://archives.datapages.com/Data/sepm/journals/v4750/data/050/050003/1010.htm>.
- Pruyers, P.A., de Lange, G.J., Middelburg, J.J., 1991. Geochemistry of eastern Mediterranean sediments: primary sediment composition and diagenetic alterations. *Marine Geology* 100, 137–154. [https://doi.org/10.1016/0025-3227\(91\)90230-2](https://doi.org/10.1016/0025-3227(91)90230-2).
- Puchelt, H., Emmermann, R., 1976. Bearing of rare earth patterns of apatites from igneous and metamorphic rocks. *Earth and Planetary Science Letters* 31 (2), 279–286. [https://doi.org/10.1016/0012-821X\(76\)90220-X](https://doi.org/10.1016/0012-821X(76)90220-X).
- Qiang, J., Cao, H., Zhang, X., et al., 2015. Geochemical characteristics of the dolomites of the Majiagou Formation in the central and eastern Ordos Basin. *Journal of Xi'an University of Science and Technology* 35 (3), 344–349. <https://doi.org/10.13800/j.cnki.xakjdxsb.2015.0312> (in Chinese).
- Read, J.F., Husinec, A., Cangialosi, M., et al., 2016. Climate controlled, fabric destructive, reflux dolomitization and stabilization via marine and synorogenic mixed fluids: an example from a large Mesozoic, calcite-sea platform, Croatia. *Palaeogeography, Palaeoclimatology, Palaeoecology* 449, 108–126. <https://doi.org/10.1016/j.palaeo.2016.02.015>.
- Sahlström, F., Arribas, A., Dirks, P., et al., 2017. Mineralogical distribution of germanium, gallium and indium at the Mt Carlton High-sulfidation epithermal deposit, NE Australia, and comparison with similar deposits worldwide. *Minerals* 7 (11), 213. <https://doi.org/10.3390/min7110213>.
- Spielhagen, R.F., Erlenkeuser, H., 1994. Stable oxygen and carbon isotopes in planktic foraminifers from Arctic Ocean surface sediments: reflection of the low salinity surface water layer. *Marine Geology* 119 (3), 227–250. [https://doi.org/10.1016/0025-3227\(94\)90183-X](https://doi.org/10.1016/0025-3227(94)90183-X).
- Stüeken, E.E., Jones, S., Raub, T.D., et al., 2020. Geochemical fingerprints of seawater in the late mesoproterozoic midcontinent rift, north America: life at the marine-land divide. *Chemical Geology* 553, 119812. <https://doi.org/10.1016/j.chemgeo.2020.119812>.
- Su, Z., Zhang, L., Li, J., et al., 2017. Characteristics of fluid inclusions in the dolomite of the ordovician Majiagou Formation in the Ordos Basin and their significance. *Bulletin of Mineralogy, Petrology and Geochemistry* 36 (5), 843–849 (in Chinese). https://kns.cnki.net/kcms/detail/detail.aspx?dbcode=CJFD&dbname=CJFDLAST2017&filename=KYDH201705018&uniplatform=NZKPT&v=7h3Gc2pVt-QpTls6VIROWqyPrhCnKJ-XYVrAdBpoCVHOUL_p0pLrA7_soMn0z
- Su, Z., Chen, A., Van Loon, A.J., et al., 2021. Depositional model and diagenetic evolution of hydrocarbon reservoirs in deep dolomites of the Ordos Basin, China. In: Yang, R., Van Loon, A.J. (Eds.), *The Ordos Basin - Sedimentological Research for Hydrocarbons Exploration*. Elsevier, Amsterdam, pp. 69–89. <https://doi.org/10.1016/B978-0-323-85264-7.0006-00>.
- Sun, R., Liu, G., Zheng, L., et al., 2010. Characteristics of coal quality and their relationship with coal-forming environment: a case study from the Zhuji exploration area, Huainan coalfield, Anhui, China. *Energy* 35 (1), 423–435. <https://doi.org/10.1016/j.energy.2009.10.009>.
- Tian, J., 2016. *Sedimentary Geochemistry*. Geological Publishing House, Beijing (in Chinese).
- Tian, W., Xiao, H., 2013. Geochemistry of the dolomite from the 5th member of the ordovician Majiagou Formation in the jingbian gas field of the Ordos Basin. *Journal of Yangtze University (nat. sci. ed.)* 10 (10), 49–55. <https://doi.org/10.16772/j.cnki.1673-1409.2013.10.011> (in Chinese).
- Valley, J.W., Kitchen, N., Kohn, M.J., et al., 1995. UWG-2, a garnet standard for oxygen isotope ratios: strategies for high precision and accuracy with laser heating. *Geochimica et Cosmochimica Acta* 59 (24), 5223–5231. [https://doi.org/10.1016/00167037\(95\)00386-X](https://doi.org/10.1016/00167037(95)00386-X).
- Wang, A., Wang, Z., Liu, J., et al., 2021. The Sr/Ba ratio response to salinity in clastic sediments of the Yangtze River Delta. *Chemical Geology* 559, 119923. <https://doi.org/10.1016/j.chemgeo.2020.119923>.
- Wang, B., Al-Aasm, I.S., 2002. Karst-controlled diagenesis and reservoir development: example from the Ordovician main-reservoir carbonate rocks on the eastern margin of the Ordos Basin, China. *AAPG Bulletin* 86 (9), 1639–1658. <https://doi.org/10.1306/61EEDD28-173E-11D7-8645000102C1865D>.
- Wang, H., 2020. Paleosedimentary environments and karst characteristics of Ordovician limestone in north China coalfields. In: Wang, H. (Ed.), *Water-resisting Property and Key Technologies of Grouting Reconstruction of the Upper Ordovician Limestone in North China's Coalfields*. Springer Theses: Springer International Publishers. https://doi.org/10.1007/978-3-030-40116-0_2.
- Wang, L., Fu, Y., Fang, S., 2018. Elemental geochemical characteristics and geological significance of Majiagou Formation, eastern Ordos Basin. *Petroleum Geology and Experiments* 40 (4), 519–525 (in Chinese). <https://kns.cnki.net/kcms/detail/detail.aspx?dbcode=CJFD&dbname=CJFDLAST2018>

- &filename=SYSD201804010&uniplatform=NZKPT&v=xPnwfThRqKDoBTCuu-OVlSkx8q_mFvHn9D_Ff-3pSS_Rims5-3mxt3Gy3-eGHP3m.
- Wang, W., Sun, Y.B., 2013. Petroleum geology and experimental analysis of the rock salt in the Majiagou Formation, eastern part of the Ordos Basin. *Science & Technology Reviews* 31 (17), 51–57 (in Chinese). https://kns.cnki.net/kcms/detail/detail.aspx?dbcode=CJFD&dbname=CJFD2013&filename=KJDB201317026&uniplatform=NZKPT&v=enmXrFh4t6v6z53cf2A5Ws2FL7Y3XDzofV3zH4JUGLc1P5LvHt0nZp_u3Hm69Mot.
- Webb, G.E., Kamber, B.S., 2000. Rare earth elements in Holocene reefal micro-bialites: a new shallow seawater proxy. *Geochimica et Cosmochimica Acta* 64 (9), 1557–1565. [https://doi.org/10.1016/S0016-7037\(99\)00400-7](https://doi.org/10.1016/S0016-7037(99)00400-7).
- Wei, W., Algeo, T.J., 2020. Elemental proxies for paleosalinity analysis of ancient shales and mudrocks. *Geochimica et Cosmochimica Acta* 287, 341–366. <https://doi.org/10.1016/j.gca.2019.06.034>.
- Wei, X., Chen, H., Zhang, D., et al., 2017. Gas exploration potential of tight carbonate reservoirs: a case study of Ordovician Majiagou Formation in the eastern Yi-Shan slope, Ordos Basin, NW China. *Petroleum Exploration and Development* 44 (3), 347–357. [https://doi.org/10.1016/S1876-3804\(17\)30041-1](https://doi.org/10.1016/S1876-3804(17)30041-1).
- Wright, J., Schrader, H., Holser, W.T., 1987. Paleoredox variations in ancient oceans recorded by rare earth elements in fossil apatite. *Geochimica et Cosmochimica Acta* 51 (3), 631–644. [https://doi.org/10.1016/0016-7037\(87\)90075-5](https://doi.org/10.1016/0016-7037(87)90075-5).
- Xiang, P., Ji, H., Shi, Y., et al., 2020. Petrographic, rare earth elements and isotope constraints on the dolomite origin of Ordovician Majiagou Formation (Jizhong Depression, North China). *Marine and Petroleum Geology* 117, 104374. <https://doi.org/10.1016/j.marpetgeo.2020.104374>.
- Xie, Q.F., Cai, Y.F., Dong, Y.P., et al., 2019. Geochemical characteristics of the Permian marine mudstone and constraints on its provenance and paleoenvironment in the Fenghai area, Fujian Province, southeastern China. *Petroleum Science* 16 (3), 527–540. <https://doi.org/10.1007/s12182-019-0313-y>.
- Xiong, Y., Tan, X., Dong, G., et al., 2020. Diagenetic differentiation in the ordovician Majiagou Formation, Ordos Basin, China: facies, geochemical and reservoir heterogeneity constraints. *Journal of Petroleum Science and Engineering* 191, 107179. <https://doi.org/10.1016/j.petrol.2020.107179>.
- Xue, H., 2018. Characteristics and genesis of buried hill dolomite reservoir of Majiagou Formation in Langgu Depression. *Fault-Block Oil and Gas Fields* 25 (5), 573–578 (in Chinese). https://kns.cnki.net/kcms/detail/detail.aspx?dbcode=CJFD&dbname=CJFDLAST2018&filename=DKYT201805007&uniplatform=NZKPT&v=dYITtnsk_PbiOMu-2gG6bHmg8f0gRIFQ-blEq0SBrrHoEKdcPccTlj6cnPmoaRZj.
- Yang, R., Fan, A., Han, Z., et al., 2017. A marine or continental nature of the deltas in the Early Cretaceous Lingshanda Formation - evidences from trace elements. *Acta Geologica Sinica (English Ed.)*, 91 (1), 367–368. <https://doi.org/10.1111/17556724.13094>.
- Yu, K., Lehmkuhl, F., Diekmann, B., Zeeden, C., et al., 2017. Geochemical imprints of coupled paleoenvironmental and provenance change in the lacustrine sequence of OrogNuur, Gobi Desert of Mongolia. *Journal of Paleolimnology* 58 (4), 511–532. <https://doi.org/10.1007/s10933-017-0007-7>.
- Zhang, H., Xu, G., Zhan, H., et al., 2021. Formation mechanisms of paleokarst and karst collapse columns of the Middle Cambrian-Lower Ordovician carbonates in Huainan coalfield, northern China. *Journal of Hydrology* 601, 126634. <https://doi.org/10.1016/j.jhydrol.2021.126634>.
- Zhang, W., Zhang, H., Ming, Q., et al., 2011. The $\delta\text{Ce}-\Sigma\text{REE}$ instruction on the sedimentary facies. *Procedia Earth and Planetary Science* 2, 334–339. <https://doi.org/10.1016/j.proeps.2011.09.052>.
- Zhao, Z., Gao, L., 1998. Standardization of δEu and δCe calculation methods. *Quality Guideline* (5), 24–26 (in Chinese). <https://kns.cnki.net/kcms/detail/detail.aspx?dbcode=CJFD&dbname=CJFD9899&filename=BZBD805.008&uniplatform=NZKPT&v=mjLZTp0FuehCspMUGI1OAE11YHjPqA8ZgFDccyG26j6BZAtK-47rgdODEPzh>.
- Zhou, Y., Bohor, B.F., Ren, Y., 2000. Trace element geochemistry of altered volcanic ash layers (tonsteins) in Late Permian coal-bearing formations of eastern Yunnan and western Guizhou Provinces, China. *International Journal of Coal Geology* 44 (3), 305–324. [https://doi.org/10.1016/S0166-5162\(00\)00017-3](https://doi.org/10.1016/S0166-5162(00)00017-3).
- Zhu, L., Zhang, G., Lee, B., et al., 2010. Zircon U-Pb dating and geochemical study of the Xianggou granite in the Ma'anqiao gold deposit and its relationship with gold mineralization. *Science China - Earth Sciences* 53 (2), 220–240. <https://doi.org/10.1007/s11430-009-0100-5>.
- Zhu, Y., Masuki, H., Hiroshi, Y., et al., 2004. Gadolinium anomaly in the distributions of rare earth elements observed for coastal seawater and river waters around Nagoya City. *Bulletin of the Chemical Society of Japan* 77 (10), 1835–1842. <https://doi.org/10.1246/bcsj.77.1835>.